ISSN: 0975-8585

Research Journal of Pharmaceutical, Biological and Chemical Sciences

A Quantum-Chemical approach toward an understanding of the Human Neutrophil Elastase inhibition by N-benzoylindazole derivatives.

Juan S. Gómez-Jeria.

Quantum Pharmacology Unit, Department of Chemistry, Faculty of Sciences, University of Chile. Las Palmeras 3425, Santiago 7800003, Chile.

ABSTRACT

We carried out an analysis of the relationships between the electronic structure and the human neutrophil elastase inhibitory capacity of a series of N-benzoylindazole derivatives. We employed a model-based method. The electronic structure of all the molecules was calculated within the Density Functional Theory at the B3LYP/6-31g(d,p) level with full geometry optimization. Linear multiple regression analysis was employed to find the best relationship between receptor binding affinity and local atomic reactivity indices belonging to a three common skeletons. The variation of the receptor binding affinity is related to the variation of a set of specific local atomic reactivity indices. The inhibitory process is orbital-controlled. A 2D partial inhibitory pharmacophore is proposed.

Keywords: Human Neutrophil Elastase, Local atomic reactivity indices, QSAR, pharmacophore, Quantum Chemistry.

Corresponding author

ISSN: 0975-8585

INTRODUCTION

Neutrophils constitute the majority of white blood cells in humans, serving as the main cellular defense against infections [1]. For the period of infection, the neutrophil life-span is extended, granulopoiesis augments, and large numbers of neutrophils arrive quickly to the sites of infection. They employ a wide array of oxygen-dependent and oxygen-independent agents to destroy infectious agents. One of the oxygen-independent mechanisms involves a 30 kDa serine protease called (human) neutrophil elastase (HNE, EC 3.4.21.37) [2, 3]. Intracellular HNE breaks down alien proteins while the extracellular HNE liberated by neutrophils, that is mostly bound to the neutrophil plasma membrane, aid neutrophil movement to infection sites by degrading several host proteins (for example, the extracellular matrix proteins). Host tissues are sheltered from harm by HNE by a number of endogenous HNE inhibitors (elafin, α_1-antitrypsin, etc.). When the equilibrium between HNE and its inhibitors is disrupted in favor of HNE, tissue damage occurs. There is evidence that points out to HNE as the key source of tissue damage in cystic fibrosis, adult respiratory distress syndrome and chronic obstructive pulmonary disease, and even to the movement of tumor cells throughout tissues [4-22]. These last facts show the need to develop therapeutic agents controlling or simply inhibiting the proteolytic activity of HNE. During the last years several groups of HNE inhibitors have been synthesized [23-43]. Among them a group of N-benzoylindazole derivatives shows promising HNE inhibitory activity [38]. With the aim to provide a first insight into the mechanisms underlying these inhibitory activities, we present here the results of a formal quantum chemical study relating electronic structure with HNE inhibitory capacity for the abovementioned compounds.

METHODS AND CALCULATIONS

The method.

The method employed is grounded in the standard statistical-mechanical definition of the equilibrium constant, K_i. After several physically-based approximations, it was shown that K_i can be expressed in terms of several atomic local reactivity indices (LARIs) [44-48]. The application of this method has produced many results proving beyond all reasonable doubt its utility [49-61]. The next step was to assume that, if the expression contains all the necessary terms to explain microscopic interactions, it can also be employed to analyze processes that are not equilibrium constants but complex biological activities (BA). The final master equation obtained is:

$$\log(\mathrm{BA}) = a + \sum_j \left[e_j Q_j + f_j S_j^E + s_j S_j^N \right] +$$
$$+ \sum_j \sum_m \left[h_j(m) F_j(m) + x_j(m) S_j^E(m) \right] + \sum_j \sum_{m'} \left[r_j(m') F_j(m') + t_j(m') S_j^N(m') \right] +$$
$$+ \sum_j \left[g_j \mu_j + k_j \eta_j + o_j \omega_j + z_j \varsigma_j + w_j Q_j^{\max} \right] + \sum_{B=1}^{W} O_B \qquad (1)$$

where a, e_j, f_j, s_j, etc., are constants to be determined. Q_j, S_j^E and S_j^N are, respectively, the net charge, the total atomic electrophilic superdelocalizability and the total atomic

nucleophilic superdelocalizability of atom j. $F_j(m)$ and $F_j(m')$ are, respectively, the Fukui index of occupied MO m and vacant MO m' of atom j [62]. $S_j^N(m')$ is the local (orbital) atomic nucleophilic superdelocalizability of vacant MO m' of atom j. $S_j^E(m)$ is the local (orbital) atomic electrophilic superdelocalizability of occupied MO m of atom j. μ_j, η_j, ω_j and ς_j are, respectively, the local atomic electronic chemical potential, the local atomic hardness, the local atomic softness and the local atomic electrophilicity of atom j. $Q_j^{\max}$ represents the maximal amount of charge atom j may receive. O_B is the orientational parameter of substituent B, a purely geometrical term derived from the rotational partition function [46]. As the physical meaning of the LARIs has been discussed in several papers, we refer the reader to the literature. The application of Eq. 1 to several different molecular systems and processes that are not equilibrium constants has given very good results [63-72]. It is important to mention that Eq. 1 includes only reactivity indices of the biologically active molecules and not their targets. Therefore, reported biological activities having an unknown or an unclear action mechanism(s) can be studied with this method. Also, and from the formal point of view, this method is the only member of a subset belonging to the set of all QSAR methods. As an example of a comparison of its potency against statistics-only-based methods we refer the reader to our paper studying the relationships between accumulation data and molecular structure for some pollutant molecules by *zucchini* subspecies [71].

Selection of experimental data.

The data selected for this study are the human neutrophil elastase (HNE) inhibitory activities, reported as the concentration of tested compound causing 50% inhibition (IC_{50}) of the enzymatic reaction of HNE with a substrate. All experimental values coming from other references were discarded. The selected molecules are shown in Fig. 1 and Table 1.

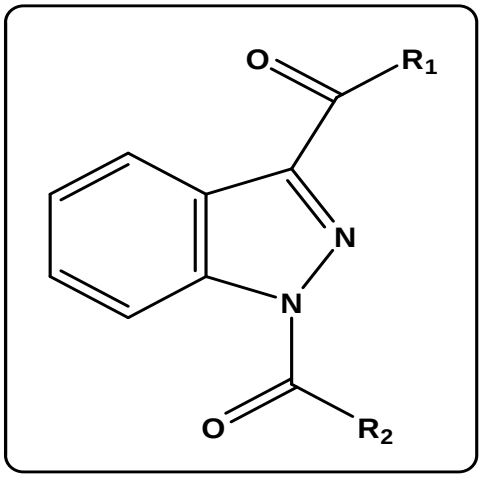

Figure 1. General formula of N-benzoylindazole derivatives.

ISSN: 0975-8585

Table 1. N-benzoylindazole derivatives and their biological activity.

Mol.	R_1	R_2	$\log(IC_{50})$
1	Phe	Phe	-0.38
2	Phe	2-Me-Phe	1.53
3	Phe	3-Me-Phe	-0.03
4	Phe	4-Me-Phe	-0.54
5	Phe	3-Cl-Phe	0.59
6	Phe	4-Cl-Phe	0.79
7	Phe	3-NO_2-Phe	1.04
8	Phe	3-F-Phe	0.77
9	Phe	4-F-Phe	0.91
10	Phe	3-OMe-Phe	0.26
11	Phe	4-CN-Phe	1.58
12	Phe	3-Thienyl	0.49
13	Phe	5-Benzodioxole	1.52
14	Phe	1-Naphthyl	1.40
15	Et	3-OMe-Phe	-0.10
16	Et	4-CN-Phe	1.58
17	Et	3-Thienyl	-0.03
18	Et	5-Benzodioxole	1.45
19	Et	Et	-0.40
20	Et	n-Pr	-0.74
21	Et	*c*-Pentyl	-0.32
22	Me	Phe	-1.05
23	Me	3-Me-Phe	-0.89
24	Me	3-OMe-Phe	-0.26
25	Me	3-Thienyl	-0.51
26	*n*-Pr	Phe	-0.40
27	*n*-Pr	3-Me-Phe	-0.11
28	*n*-Pr	3-OMe-Phe	0.28
29	*n*-Pr	3-Thienyl	0.28
30	i-Pr	Phe	-0.62
31	i-Pr	3-Me-Phe	-0.19
32	i-Pr	3-OMe-Phe	-0.12
33	i-Pr	3-Thienyl	-0.16
34	n-CH_2CF_3	Phe	-0.59
35	n-CH_2CF_3	3-Me-Phe	-0.34
36	n-CH_2CF_3	3-OMe-Phe	-0.05
37	n-CH_2CF_3	3-Thienyl	-0.29
38	Phe	3-NH_2-Phe	0.49
39	Et	3-NH_2-Phe	0.20
40	n-Pr	3-NH_2-Phe	-0.15
41	i-Pr	3-NH_2-Phe	-0.29
42	n-CH_2CF_3	3-NH_2-Phe	-0.47

Calculations

If we consider a series of n molecules, we have a set of n Eqs. 1. The direct resolution of this linear system of equations is possible only if we have enough molecules to solve it. Unhappily this is never the real situation. Therefore we must rely on linear multiple regression analysis (LMRA) techniques to find the best solution. The problem with LMRA is

ISSN: 0975-8585

that the resulting equations will include only those LARIs whose variation accounts for the variation of the experimental values through the series. Then, atoms participating in the process but having a constant value of all their LARIs throughout the series of molecules will not appear in the final equations. This apparent shortcoming has not prevented us from suggesting possible molecules with stronger biological activities. This is the case of a potent hallucinogen (successful) and a stronger cannabinoid (not tested). We were even able to detect wrong experimental results. The electronic structure of all molecules in Table 1 was obtained within the Density Functional Theory at the B3LYP/6-31G(d,p) level with the Gaussian program [73]. After full geometry optimization, the local atomic reactivity indices were obtained with the D-CENT-QSAR software [74].

For the LMRA we made the following assumption: there is a set of atoms, common to all molecules (called the common skeleton, CS), that accounts for almost all the biological activity. The common skeleton definition depends on the concrete problem being studied. Here we tested three possible CSs (see below). Then, the matrices for LMRA are constituted by the logarithm of IC_{50} (the dependent variable) and the set of LARIs of each one of the common skeletons used. The Statistica software was employed [75]. The drawings of the molecular electrostatic potential (MEP) and the molecular orbitals were done with Molekel and GaussView programs [76, 77].

RESULTS

First, we carried out a LMRA with the whole set of molecules (n=42) using the common skeleton depicted in Fig. 1 (CS-A).

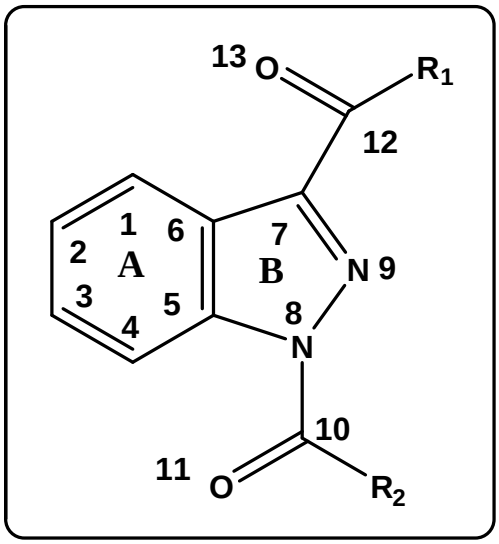

Figure 2. Common skeleton of N-benzoylindazole derivatives (CS-A).

The results showed that molecules 2, 8 and 16 appeared as outliers. The next LMRA with these three molecules discarded (n=39), produced the following statistically significant equation:

$$\log(IC_{50}) = -4.23 + 0.001\phi_2 - 8.74Q_9 - 1.29F_6(LUMO+1)^* \quad (2)$$

ISSN: 0975-8585

with n=39, R=0.89, R^2=0.80, adj R^2=0.78, F(3,35)=46.92 (*p<0.00001*) and SD=0.31. No outliers were detected and no residuals fall outside the ±2σ limits. Here Q_9 is the net charge of atom 9, ϕ_2 is the orientational parameter of R_2 and $F_6(LUMO+1)^*$ is the Fukui index of the second local vacant MO localized on atom 6. Tables 2 and 3 show, respectively, the beta coefficients, the results of the t-test for significance of coefficients and the matrix of squared correlation coefficients for the variables appearing in Eq. 2. Table 3 shows that no significant internal correlations between independent variables exist. Figure 3 displays the plot of observed *vs.* calculated values. The associated statistical parameters of Eq. 2 show that this equation is statistically significant and that the variation of a group of local atomic reactivity indices belonging to the type A common skeleton explains about 78% of the variation of the HNE inhibition.

Table 2: Beta coefficients and *t*-test for significance of the coefficients in Eq. 2.

	Beta	t(35)	p-level
ϕ_2	0.70	8.90	0.000001
Q_9	-0.33	-4.17	0.0002
$F_6(LUMO+1)^*$	-0.29	-3.76	0.0006

Table 3: Squared correlation coefficients for the variables appearing in Eq. 2.

	$F_6(LUMO+1)^*$	Q_9
Q_9	0.03	1.00
ϕ_2	0.01	0.06

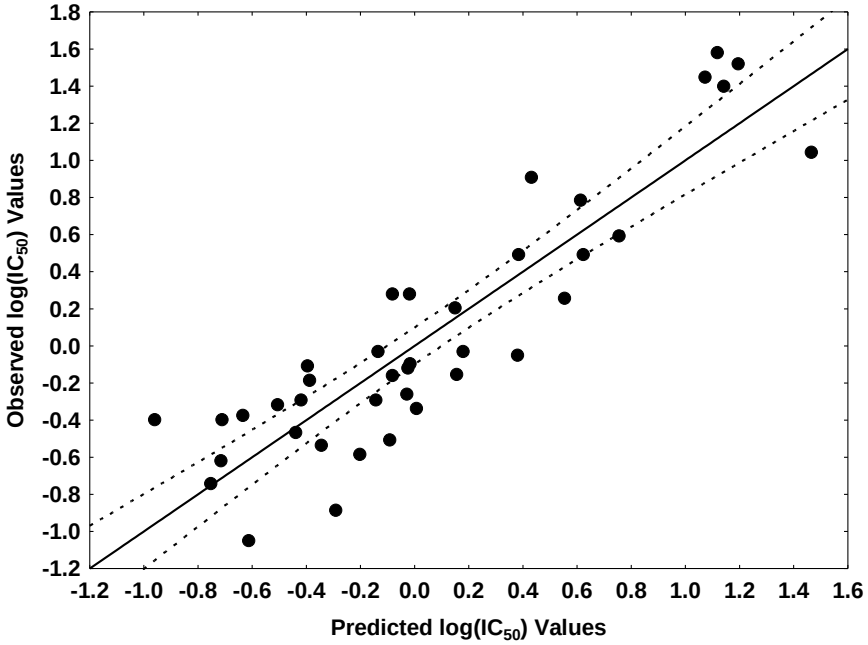

Figure 3: Observed *vs.* predicted values (Eq. 2) of log (IC_{50}). Dashed lines denote the 95% confidence interval.

ISSN: 0975-8585

The SD value of Eq. 2 is high for our standards (0.31). On the other hand, Fig. 3 clearly shows that there are many points located far from the 95% confidence interval. Now, if we examine the list of molecules, we can see that there is a group of them having aromatic substituents as R_1 and R_2 (molecules 1-14 and 38 in Table 1). To examine the possibility that one or both aromatic systems participate in the inhibitory process we generated the common skeleton B, shown in Fig. 4. All molecules having only phenyl substituents at R_1 and R_2 were included in this set.

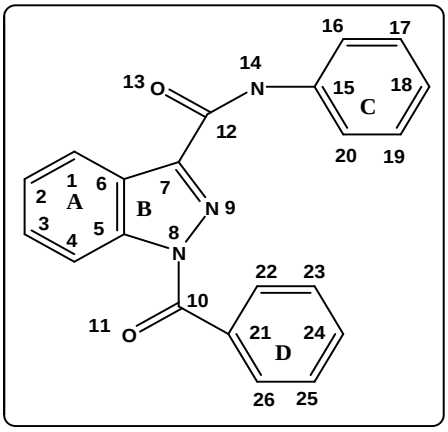

Figure 4. Common skeleton of N-benzoylindazole derivatives (CS-B).

For this set the following statistically significant equation was obtained:

$$\log(IC_{50}) = 49.08 + 87.37S_{11}^{E} + 5.02F_6(HOMO-2)^* - 2.03F_{16}(LUMO+1)^* \quad (3)$$

with n=12, R=0.94, R^2=0.89, adj R^2=0.84, F(3,8)=20.59 (*p<0.0004*) and SD=0.27. No outliers were detected and no residuals fall outside the ±2σ limits. Here S_{11}^{E} is the total atomic nucleophilic superdelocalizability of atom 11, $F_6(HOMO-2)^*$ is the Fukui index of the third highest occupied local MO localized on atom 6 and $F_{16}(LUMO+1)^*$ is the Fukui index of the second lowest vacant local MO localized on atom 16. Tables 4 and 5 show, respectively, the beta coefficients, the results of the t-test for significance of coefficients and the matrix of squared correlation coefficients for the variables appearing in Eq. 3. Table 4 shows that no significant internal correlations between independent variables exist. Figure 5 displays the plot of observed *vs.* calculated values. The associated statistical parameters of Eq. 3 show that this equation is statistically significant and that the variation of a group of local atomic reactivity indices belonging to the type B common skeleton explains about 84% of the variation of the HNE inhibition.

Table 4: Beta coefficients and *t*-test for significance of the coefficients in Eq. 3.

	Beta	t(8)	p-level
S_{11}^{E}	1.40	6.84	0.0001
$F_6(HOMO-2)^*$	0.84	4.74	0.001
$F_{16}(LUMO+1)^*$	-0.64	-3.10	0.01

ISSN: 0975-8585

Table 5: Squared correlation coefficients for the variables appearing in Eq. 3.

	S_{11}^{E}	$F_6(HOMO-2)^*$
$F_6(HOMO-2)^*$	0.11	1.00
$F_{16}(LUMO+1)^*$	0.34	0.12

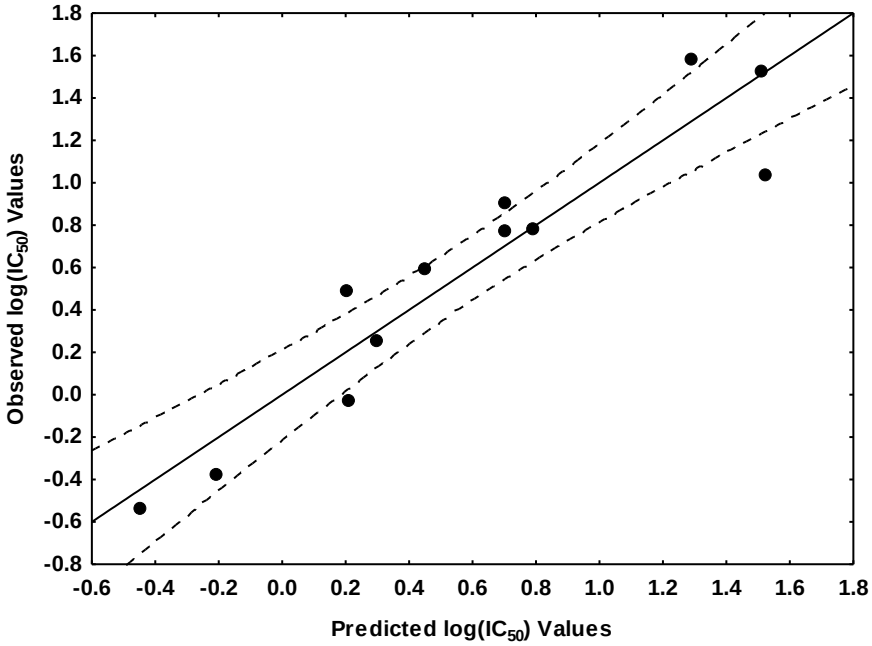

Figure 5: Observed *vs.* predicted values (Eq. 3) of log (IC_{50}). Dashed lines denote the 95% confidence interval.

Also we carried out an extra LMRA including the orientational parameters for the substituents of the R_2 phenyl ring but no statistically significant results were obtained.

The last group of molecules is constituted by those having a non-aromatic substituent at R_1 and an aromatic one at R_2. The associated common skeleton, CS-C, is shown in Fig. 6. Molecules having an aromatic substituent at R_2 that is not a phenyl ring were discarded.

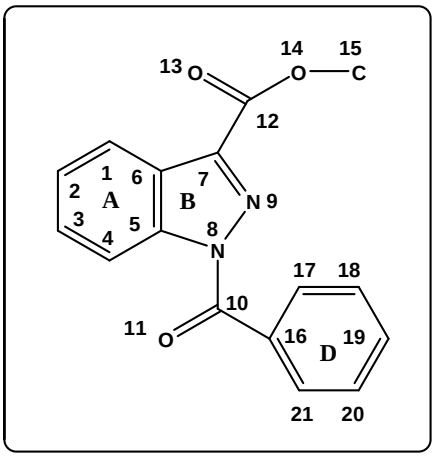

Figure 6. Common skeleton of N-benzoylindazole derivatives (CS-C).

For this case we obtained the following statistically significant equation:

$$\log(IC_{50}) = 67.11 - 2.62S_2^N(LUMO+1)^* + 13.48S_{20}^E(HOMO-1)^* + 654.02Q_3 \quad (4)$$

with n=18, R=0.96, R^2=0.92, adj R^2=0.91, F(3,14)=57.43 (*p<0.000001*) and SD=0.17. No outliers were detected and no residuals fall outside the ±2σ limits. Here Q_3 is the net charge of atom 3, $S_2^N(LUMO+1)^*$ is the orbital atomic nucleophilic superdelocalizability of the second local vacant MO localized on atom 2 and $S_{20}^E(HOMO-1)^*$ is the orbital atomic electrophilic superdelocalizability of the second highest occupied local MO localized on atom 20.

Tables 6 and 7 show, respectively, the beta coefficients, the results of the t-test for significance of coefficients and the matrix of squared correlation coefficients for the variables appearing in Eq. 4. Table 7 shows that no significant internal correlations between independent variables exist. Figure 7 displays the plot of observed *vs.* calculated values. The associated statistical parameters of Eq. 4 show that this equation is statistically significant and that the variation of a group of local atomic reactivity indices belonging to the C type common skeleton explains about 91% of the variation of the HNE inhibition.

Table 6: Beta coefficients and *t*-test for significance of the coefficients in Eq. 4.

	Beta	t(14)	p-level
$S_2^N(LUMO+1)^*$	-0.70	-7.97	0.000001
$S_{20}^E(HOMO-1)^*$	0.57	6.79	0.000009
Q_3	0.42	4.27	0.0007

Table 7: Squared correlation coefficients for the variables appearing in Eq. 4.

	$S_2^N(LUMO+1)^*$	Q_3
Q_3	0.29	1.00
$S_{20}^E(HOMO-1)^*$	0.03	0.23

In the analysis of other biological activities, we found that the elimination of the highest experimental values for the LRMA produced statistically significant equations. This was explained by suggesting that, within a given range of experimental values, there was only one mechanism of action and that higher values could reflect a change in the action mechanism, a saturation effect, or both. For this case a LMRA was carried out without including those molecules having log(IC_{50}) > 0.9. No statistically significant results were obtained, suggesting that all molecules studied here have the same general action mechanism.

ISSN: 0975-8585

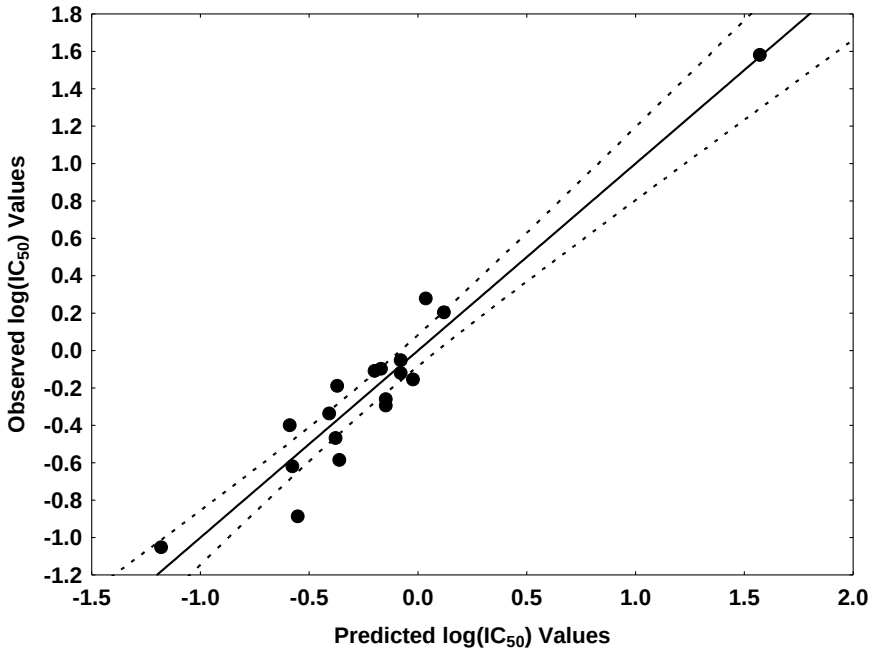

Figure 7: Observed *vs.* predicted values (Eq. 4) of log (IC_{50}). Dashed lines denote the 95% confidence interval.

DISCUSSION

Molecular Electrostatic Potentials (MEP).

If molecules exercise their inhibitory activities at the same site and through the same mechanism, we expect that their MEP's should be similar for the recognition process to occur. Figure 8 displays the MEP of molecules 4, 15, 20 and 11 (see Table 1).

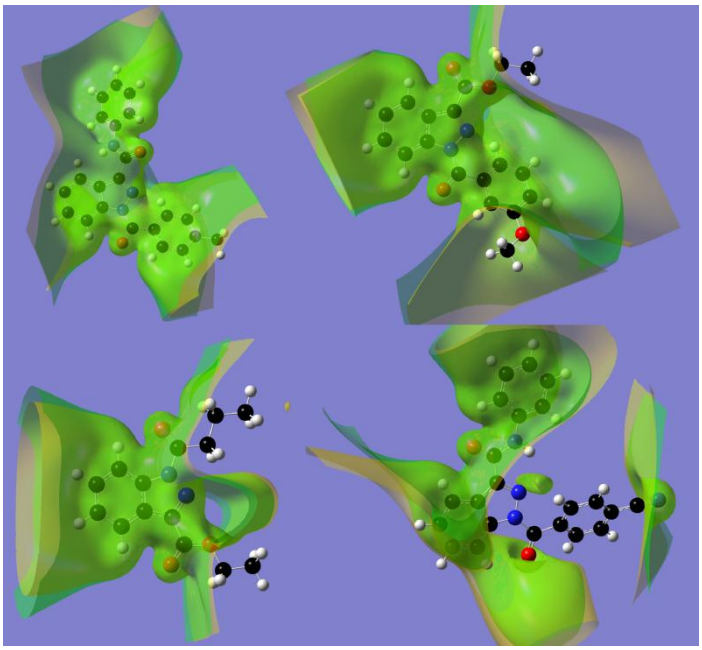

Figure 8. MEP of molecules 4 (upper left), 15 (upper right), 20 (lower left) and 11 (lower right). The green isovalue surface corresponds to negative MEP values (-0.01) and the yellow isovalue surface to positive MEP values (0.01).

ISSN: 0975-8585

We can see that the structures are very different, preventing us even from making qualitative statements about MEP structure and inhibitory potency. Given that the R_1 and R_2 substituents have conformational flexibility we can expect that in the experimental setup in which the measurements were carried out any given molecule will have a distribution of conformers and hence of MEPs. Some of these conformers may be active, but the experimental data used here do not allow us to identify the active ones. Perhaps the synthesis and testing of similar but conformationally restricted compounds can shed light on this problem. On the other hand, the MEP at a greater distance is a valuable tool for analyzing the process of guiding the molecule to its interaction site. Figure 8 shows the MEP of molecules 4, 15, 20 and 11 at a distance of 3.5 Å from the nuclei (see Table 1).

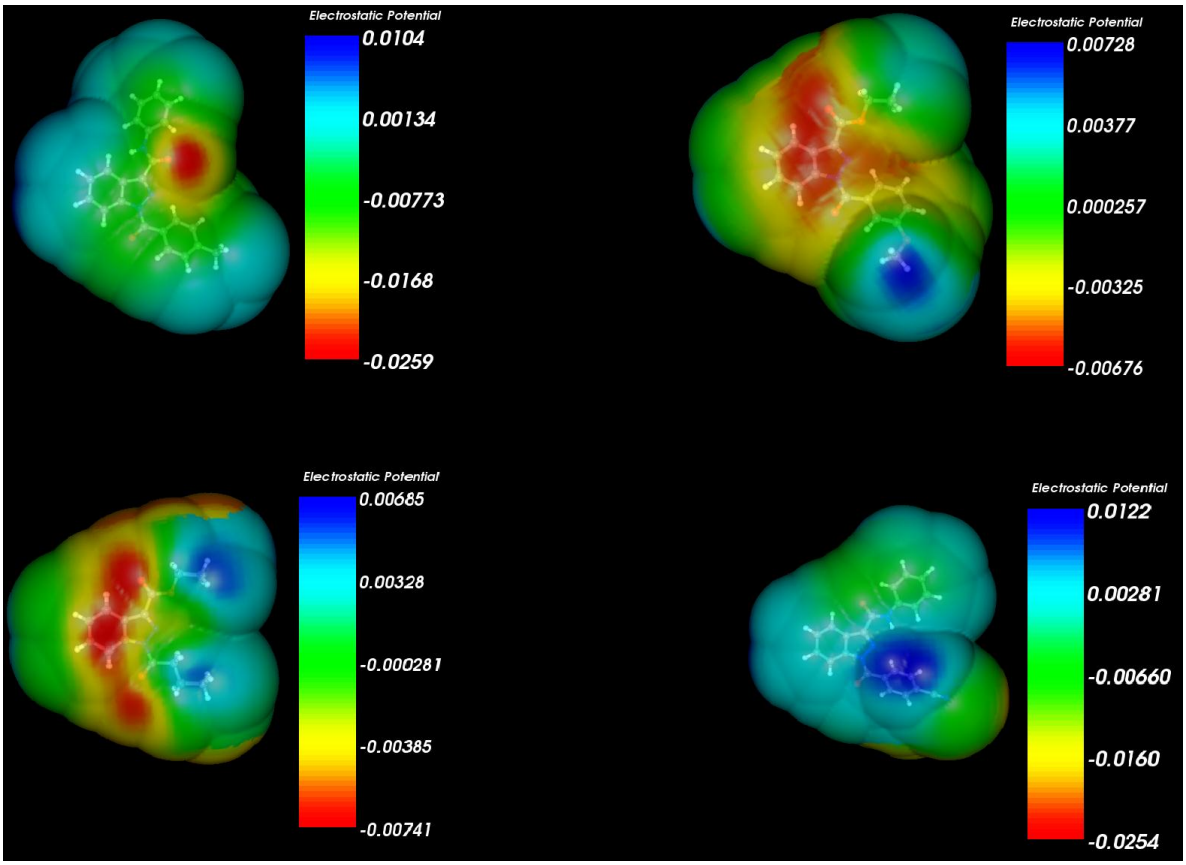

Figure 9. MEP of molecules 4 (upper left), 15 (upper right), 20 (lower left) and 11 (lower right) at a distance of 3.5 Å from the nuclei.

We can see that all these MEPs are similar in their general shape but not in the distribution of negative and positive MEP regions. Then, if MEPs are related to the guiding process, in this specific case we are not able to detect what general shape is adequate. This situation should appear only in large molecules with conformational flexibility, but this is the first time we find it so markedly. The origin of this can be directly tracked to the fact that all calculations are done for the fully optimized molecules *in vacuo* and that these conformations are not necessarily the active ones. In the future we envisage two lines of research to tackle this question. The first one is to fully optimize geometries in presence of a solvent (simulated or explicit). The second works only if and only if we have at least one fully conformationally restricted active molecule in the set analyzed. It consists in superimposing the molecules with conformational flexibility on the rigid one.

ISSN: 0975-8585

Molecular Orbitals and Local Molecular Orbitals.

Here we shall discuss some aspects of MO localization on these molecules and introduce the concept of Local Molecular Orbitals (LMO). In large molecules, where two or more conjugated regions coexist, the frontier molecular orbitals (FMO, HOMO and LUMO) or other MOs can be localized in several different ways. Figure 10 shows the HOMOs of molecules 2, 3, 19 and 42.

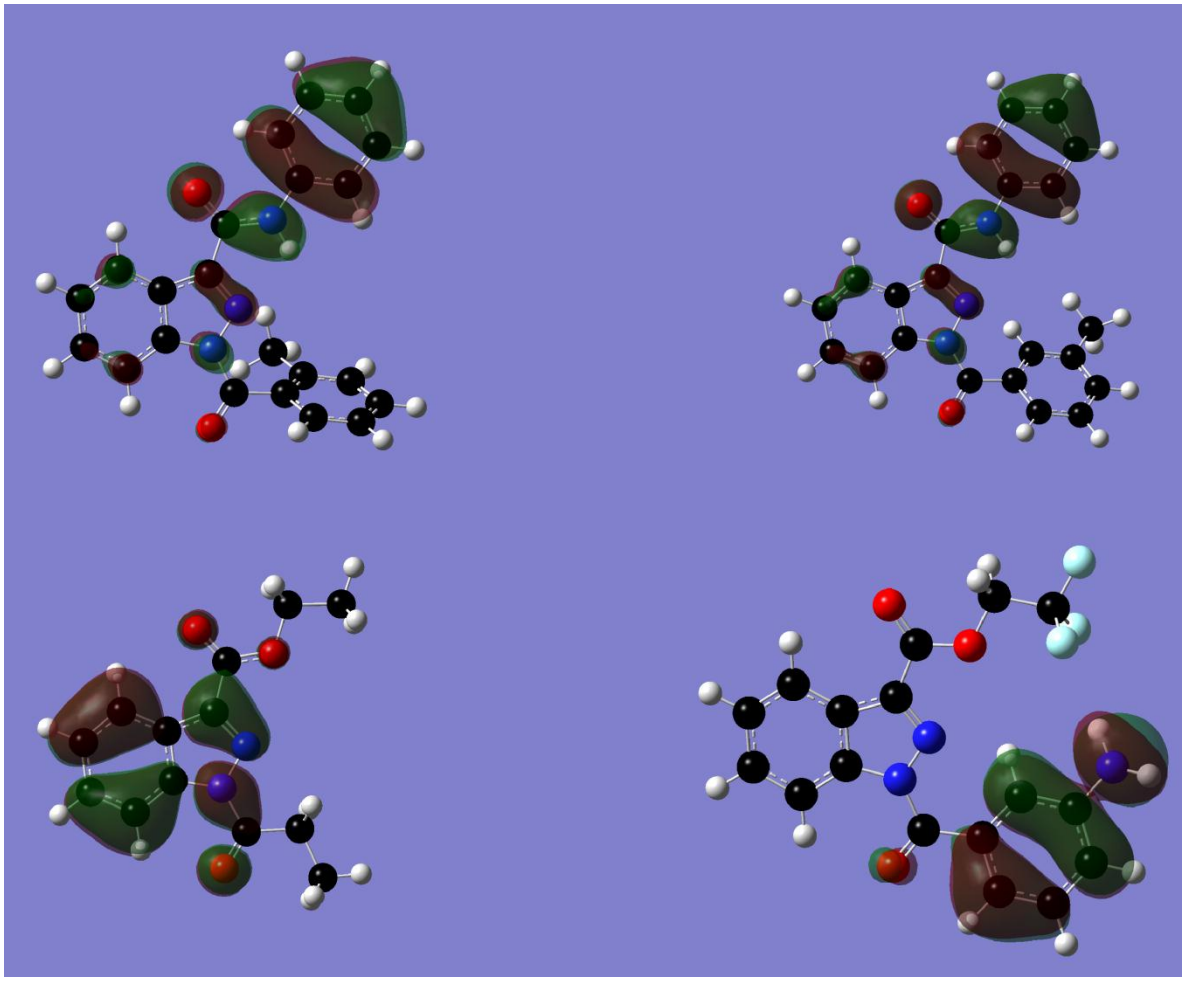

Figure 10. Localization of the molecular HOMO in molecules 2, 3, 19 and 42 (isovalue=0.02).

We can see that in molecules 2 and 3 the HOMO is localized mainly on the R_1 phenyl substituent and on the indazole fragment. In molecule 19 the HOMO is localized on the indazole fragment. Finally, in molecule 42 the HOMO is localized on the R_2 phenyl ring. Now, let us suppose that the indazole fragment acts as an electron donor in a π-π stacking interaction (or, in general, with an electron-deficient area). In the case of molecules 2, 3 and 19 this will occur through the molecular HOMO, but in the case of molecule 42 this process will take place through the highest occupied π MO that does not coincide with the molecular HOMO. More precisely, the highest occupied π MO of molecule 42 is the second highest occupied MO of this molecule (called HOMO-1). To represent these facts we have defined the following nomenclature. The highest occupied MO localized on one atom is called its local HOMO and is written as HOMO*. It may coincide or not with the molecular HOMO. The next occupied MO localized on an atom is called (HOMO-1)*, and so on. The

ISSN: 0975-8585

case of vacant MOs is similar: LUMO* designs the lowest vacant MO localized on an atom, (LUMO+2) the second lowest vacant MO localized on an atom, etc. This nomenclature is used below. Figure 11 shows the localization of the molecular LUMO in molecules 2, 3, 19 and 42.

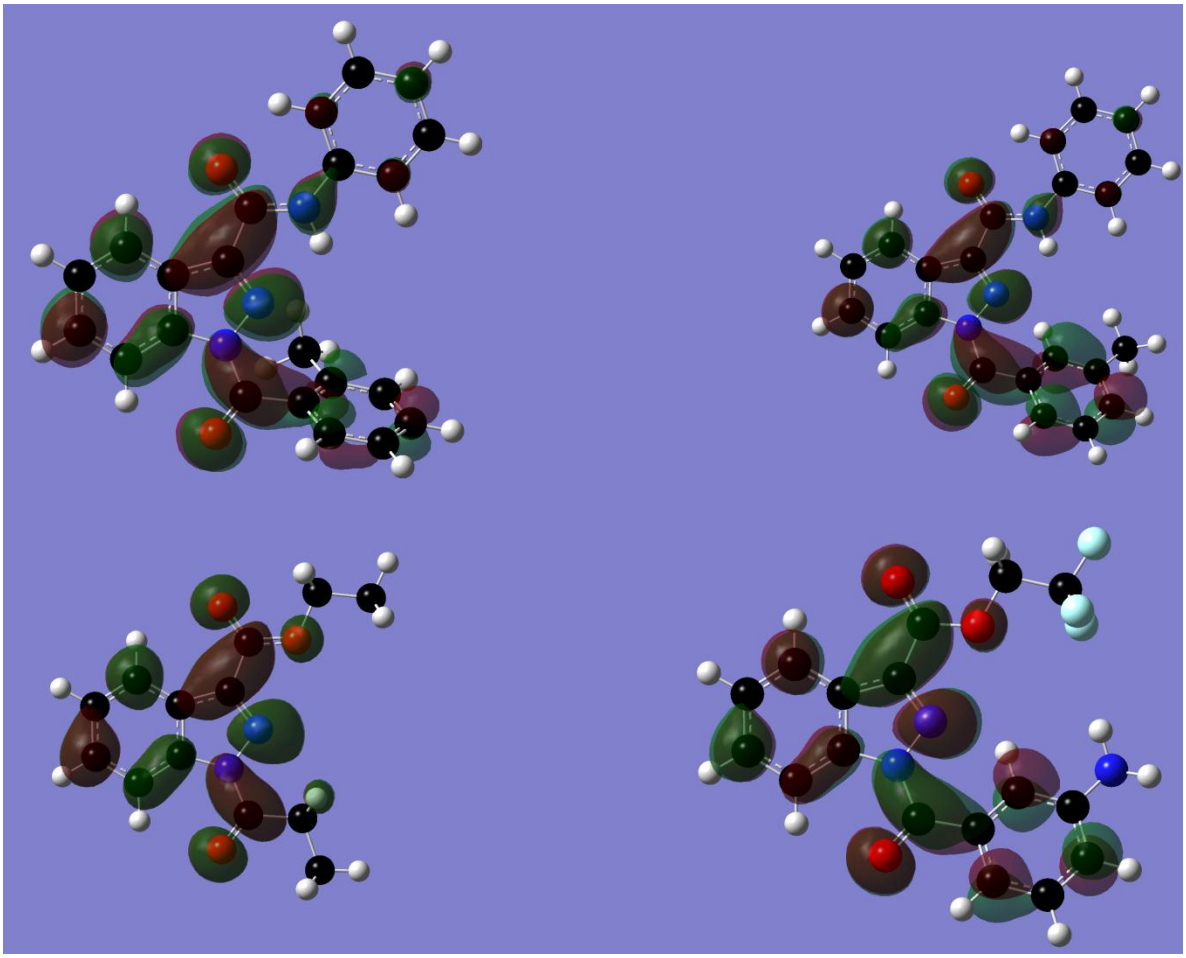

Figure 11. Localization of the molecular LUMO in molecules 2, 3, 19 and 42 (isovalue=0.02).

We can now see that the LUMO is localized on the indazole moiety in all four molecules. In the case of molecules 2, 3 and 42 the LUMO is also localized on several atoms of the R_2 phenyl substituent. Using the nomenclature for local MOs we can see in Fig. 11 that the (LUMO)* for any atom of the R_1 phenyl substituent for the cases of molecules 2 and 3 will not coincide with the molecular LUMO.

Relationships between electronic structure and HNE inhibitory activity.

Our results show that, for each common skeleton analyzed, the variation of log(IC_{50}) is associated with the variation of the value of several local atomic reactivity indices located on them. In Eq. 2 we must add the orientational parameter of one substituent.

The beta values (Tables 2, 4 and 6) show that the importance of variables within each equation is the following:

Eq. 2: $\phi_2 > Q_9 > F_6(LUMO+1)^*$.

ISSN: 0975-8585

Eq. 3: S_{11}^{E} > $F_6(HOMO-2)^*$ > ($F_{16}(LUMO+1)^*$).

Eq. 4: $S_2^N(LUMO+1)^*$ > $S_{20}^{E}(HOMO-1)^*$ > Q_3 .

Before proceeding to the analysis we must mention that, as we assumed that these molecules have a similar mechanism of action, the results obtained in Eqs. 2 to 4 must not be contradictory.

A variable-by-variable analysis of Eq. 2 indicates that a high inhibitory capacity is associated with a small value for ϕ_2, a negative value for Q_9 and a high value for $F_6(LUMO+1)^*$. A small value for ϕ_2, a strictly geometrical parameter, suggests that an aromatic moiety smaller than a phenyl group, such as a thienyl substituent, will be optimal as ring D. A negative value for the net charge of atom 9 (a nitrogen atom in ring B) is normally present in the molecules studied here. The question is only what to do to raise its negative value. The appearance of a net charge suggests an electrostatic interaction with a center located in the partner. A high value for $F_6(LUMO+1)^*$ suggests that atom 6 (belonging to rings A and B) interacts with an electron-rich area of the site. This interaction occurs through its local LUMO* and (LUMO+1)*. Both MOs are of π nature in all molecules.
A variable-by-variable analysis of Eq. 3 indicates that a high inhibitory capacity is associated with a small value for $F_6(HOMO-2)^*$ and high values for S_{11}^{E} and $F_{16}(LUMO+1)^*$. A high value for S_{11}^{E} suggests that atom 11 is strongly interacting with an electron-acceptor site. Let us remember that a total atomic electrophilic superdelocalizability is a summation over all occupied MOs of terms with the form $F_i(MO_r)^*/E(MO_r)$, where E(MO_r) is the eigenvalue associated to the r-th MO. The most important terms of this summation are the ones corresponding to the first occupied MOs. This fact points to a directional interaction, such as a hydrogen bonding with the partner. The local $(HOMO-2)_6^*$ is of π nature in some molecules and of σ nature in others. As Eq. 2 suggests that atom 6 is interacts with an electron-rich center, so that a low value for the electron populations of the local (HOMO-2)* of atom 6, especially of those of σ nature, will facilitate the interaction. In Table 8 we present the Fukui indices and nature of the three highest occupied and two lowest vacant local MOs of atom 6 in some molecules.

Table 8: Fukui indices and nature of some local MOs of atom 6.

Molecule	(HOMO-2)*	(HOMO-1)*	HOMO*	LUMO*	(LUMO+1)*
1	0.09 (π)	0.26 (π)	0.01 (π)	0.05 (π)	0.10 (π)
6	0.27 (π)	0.07 (π)	0.01 (π)	0.04 (π)	0.10 (π)
17	0.04 (π)	0.02 (π)	0.44 (π)	0.05 (π)	0.04 (π)
36	0.20 (π)	0.23 (π)	0.01 (π)	0.02 (π)	0.02 (π)
42	0.03 (σ)	0.31 (π)	0.12 (π)	0.02 (π)	0.35 (π)

We can see that not all the molecules have a high value of $F_6(LUMO+1)^*$ and that $F_6(LUMO)^*$ is low in all of them. With this information we may say that the main component of the interaction of atom 6 with an electron-rich counterpart is its (LUMO+1)*. On the other hand, we expect that the electron populations of the HOMO* and (HOMO-1)* should be low to minimize the repulsive interaction between the occupied MOs of atom 6

and the site. We may see in Table 8 that only molecule 17 fulfills this condition and also the condition of a low electron population at the (HOMO-2)* level. The condition of a high value for $F_{16}(LUMO+1)^*$ must be considered with caution due to its low p-value (Table 4). The two lowest vacant MOs of atom 16 are of π nature. Then, we may suggest that atom 16 is interacting with an electron-rich area of the partner. Note that atom 16 belongs to ring C (see Fig. 4) that is not common to all the molecules analyzed here. Therefore it is possible to suggest the existence of an extra site available to some but not all inhibitors.

A variable-by-variable analysis of Eq. 4 indicates that a high inhibitory capacity is associated with small values for $S_2^N(LUMO+1)^*$, a negative value for Q_3 and a high value for $S_{20}^E(HOMO-1)^*$. In all molecules the net charge of atom 3, Q_3, has a negative value. The challenge is to try substituents enhancing this negative value while maintaining the negative charge of atom 9 and without altering the MO's nature and localization on atom 6. Atom 3 seems to interact electrostatically with a positive center of the partner. A high value for $S_{20}^E(HOMO-1)^*$ indicates that atom 20 (belonging to ring D, Fig. 4) might be interacting with an electron-deficient center of the partner through its two highest occupied MOs (both MOs are of π nature). The analysis of $S_2^N(LUMO+1)^*$ is still a complex problem due to the fact that the (LUMO+1)* associated eigenvalue is negative, a usual problem found in DFT and Hartree-Fock calculations. The requirement is that $S_2^N(LUMO+1)^*$ be numerically small. We can obtain this result by diminishing the electron population of this MO, by further lowering the associated negative eigenvalue (the (LUMO+1)* approaches the LUMO*) or by both manipulations. Within this approach we may interpret this requirement by suggesting that atom 2 is interacting with an electron-rich center located in the partner. Let us suppose now that the associated eigenvalue is positive. In this case the requirement is that $S_2^N(LUMO+1)^*$ should have a high value. This can be obtained by lowering the electron population of this MO, by lowering the associated positive eigenvalue (also the (LUMO+1)* approaches the LUMO*) or in both ways simultaneously. Then, this interpretation seems to be correct.

All the suggestions resulting from the above results are depicted in the partial two-dimensional (2D) inhibition pharmacophore depicted in Fig. 12.

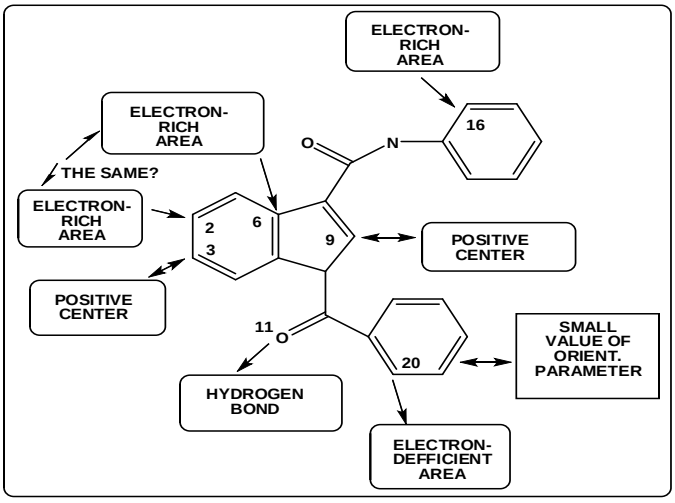

Figure 12. Partial 2D pharmacophore for the inhibition of HNE by N-benzoylindazole derivatives.

It is important to mention that we use the term "partial" for the pharmacophore because the information that it includes is not necessarily complete. For example, when we suggest that atom 20 is interacting with an electron-deficient area, we cannot determine if this atom interacts directly with an atom of the partner on its own, or if it is engaged together with other atoms of its ring in a π-π stacking interaction. The resulting equations show that the inhibition process has a high degree of orbital control [78]. This implies that this inhibition has a very high degree of specificity resulting from a long evolutionary process leading to the protection of living systems from their chemical environment.

CONCLUSIONS

Good quality quantitative structure-activity relationships were obtained for the inhibition of human neutrophil elastase by N-benzoylindazole derivatives. The process has a high degree of orbital control. An extra site, not avaliable for all molecules, was detected. A putative 2D inhibition pharmacophore is proposed.

ACKNOWLEDGEMENTS

Prof. Dr. Bruce K. Cassels (Faculty of Sciences, University of Chile) is thanked for helpful comments.

REFERENCES.

[1] Garcia, RC, Peterson, CGB, Segal, AW, Venge, P. Biochem. Biophys. Res. Comm., 1985, 132, 1130-1136.
[2] Sinha, S, Watorek, W, Karr, S, Giles, J, Bode, W, Travis, J. Proc. Natl. Acad. Sci. USA, 1987, 84, 2228-2232.
[3] Navia, MA, McKeever, BM, Springer, JP, Lin, TY, Williams, HR, Fluder, EM, Dorn, CP, Hoogsteen, K. Proc. Natl. Acad. Sci. USA, 1989, 86, 7-11.
[4] Pipoly, DJ, Crouch, EC. Biochem., 1987, 26, 5748-5754.
[5] Kanayama, N, Terao, T, Horiuchi, K. Asia-Oc. J. Obst. Gyn., 1988, 14, 389-397.
[6] Okada, Y, Nakanishi, I. FEBS Lett., 1989, 249, 353-356.
[7] Nortier, J, Vandenabeele, P, Noël, E, Bosseloir, Y, Goldman, M, Deschodt-Lanckman, M. Life Sci., 1991, 49, 1879-1886.
[8] Kittelberger, R, Neale, TJ, Francky, KT, Greenhill, NS, Gibson, GJ. Biochem. Bioph. Acta Mol. Bas. Dis., 1992, 1139, 295-299.
[9] Bykowska, K, Duk, M, Kuσnierz-Alejska, G, Kopeć, M, Lisowska, E. Brist. J. Haematol., 1993, 84, 736-742.
[10] Cabanis, A, Gressier, B, Brunet, C, Dine, T, Luyckx, M, Cazin, M, Cazin, JC. Gen. Pharmacol. Vasc. Syst., 1996, 27, 1409-1414.
[11] Hiyama, A, Takeda, J, Kotake, Y, Morisaki, H, Fukushima, K. J. Cardiothor. Vasc. Anesth., 1997, 11, 580-584.
[12] Wyatt, JP, Robertson, CE. Resuscit., 1997, 34, 190.
[13] Bach-Gansmo, ET, Godal, HC, Skjønsberg, OH. Thromb. Res., 1998, 92, 125-134.

[14] Reid, PT, Marsden, ME, Cunningham, GA, Haslett, C, Sallenave, JM. FEBS Lett., 1999, 457, 33-37.
[15] Imamura, T, Tanase, S, Hayashi, I, Potempa, J, Kozik, A, Travis, J. Biochem. Biophys. Res. Comm., 2002, 294, 423-428.
[16] Ishikawa, S, Takai, E, Tamori, Y, Egami, H, Ogawa, M. Int. Congr. Ser., 2003, 1255, 243-248.
[17] Huang, C-D, Chen, H-H, Wang, C-H, Chou, C-L, Lin, S-M, Lin, H-C, Kuo, H-P. Life Sci., 2004, 74, 2479-2492.
[18] Tamakuma, S, Ogawa, M, Aikawa, N, Kubota, T, Hirasawa, H, Ishizaka, A, Taenaka, N, Hamada, C, Matsuoka, S, Abiru, T. Pulm. Pharmacol. Ther., 2004, 17, 271-279.
[19] Ujiie, Y, Oida, S, Gomi, K, Arai, T, Fukae, M. J. Periodont. res., 2007, 42, 325-330.
[20] Lee, H-H, Sung, M-H. Cell Biochem. Funct., 2013, 31, 305-311.
[21] Gifford, AM, Chalmers, JD. Curr. Op. Hematol., 2014, 21, 16-22.
[22] Malech, H, DeLeo, F, Quinn, M, "The Role of Neutrophils in the Immune System: An Overview," in *Neutrophil Methods and Protocols*, M. T. Quinn, and F. R. DeLeo Eds., vol. 1124, pp. 3-10, Humana Press, 2014.
[23] Nakao, A, Partis, RA, Jung, GP, Mueller, RA. Biochem. Biophys. Res. Comm., 1987, 147, 666-674.
[24] Trainor, DA. Trends Pharmacol. Sci., 1987, 8, 303-307.
[25] Miyano, M, Deason, JR, Nakao, A, Stealey, MA, Villamil, CI, Sohn, DD, Mueller, RA. J. Med. Chem., 1988, 31, 1052-1061.
[26] Mehdi, S, Angelastro, MP, Burkhart, JP, Koehl, JR, Peet, NP, Bey, P. Biochem. Biophys. Res. Comm., 1990, 166, 595-600.
[27] Kawabata, K, Suzuki, M, Sugitani, M, Imaki, K, Toda, M, Miyamoto, T. Biochem. Biophys. Res. Comm., 1991, 177, 814-820.
[28] Sommerhoff, CP, Krell, RD, Williams, JL, Gomes, BC, Strimpler, AM, Nadel, JA. Eur. J. Pharmacol., 1991, 193, 153-158.
[29] Bluhm, A. J. Oral Maxillofac. Surg., 1992, 50, 1020.
[30] Cunningham, RT, Mangold, SE, Spruce, LW, Ying, QL, Simon, SR, Wieczorek, M, Ross, S, Cheronis, JC, Kirschenheuter, GP. Bioorg. Chem., 1992, 20, 345-355.
[31] Edwards, PD, Wolanin, DJ, Andisik, DW, Davis, MW. J. Med. Chem., 1995, 38, 76-85.
[32] Toth, I, Christodoulou, M, Bankowsky, K, Flinn, N, Gibbons, WA, Godeau, G, Moczar, E, Hornebeck, W. Int. J. Pharmaceut., 1995, 125, 117-122.
[33] Cregge, RJ, Durham, SL, Farr, RA, Gallion, SL, Hare, CM, Hoffman, RV, Janusz, MJ, Kim, H-O, Koehl, JR, Mehdi, S, Metz, WA, Peet, NP, Pelton, JT, Schreuder, HA, Sunder, S, Tardif, C. J. Med. Chem., 1998, 41, 2461-2480.
[34] Schepetkin, IA, Khlebnikov, AI, Quinn, MT. J. Med. Chem., 2007, 50, 4928-4938.
[35] Huang, W, Yamamoto, Y, Li, Y, Dou, D, Alliston, KR, Hanzlik, RP, Williams, TD, Groutas, WC. J. Med. Chem., 2008, 51, 2003-2008.
[36] Steinbrecher, T, Hrenn, A, Dormann, KL, Merfort, I, Labahn, A. Bioorg. Med. Chem., 2008, 16, 2385-2390.
[37] Shreder, KR, Cajica, J, Du, L, Fraser, A, Hu, Y, Kohno, Y, Lin, ECK, Liu, SJ, Okerberg, E, Pham, L, Wu, J, Kozarich, JW. Bioorg. Med. Chem. Lett., 2009, 19, 4743-4746.
[38] Crocetti, L, Giovannoni, MP, Schepetkin, IA, Quinn, MT, Khlebnikov, AI, Cilibrizzi, A, Piaz, VD, Graziano, A, Vergelli, C. Bioorg. Med. Chem., 2011, 19, 4460-4472.
[39] Madsen, JLH, Andersen, TL, Santamaria, S, Nagase, H, Enghild, JJ, Skrydstrup, T. J. Med. Chem., 2012, 55, 7900-7908.

[40] Winiarski, Ł, Oleksyszyn, J, Sieńczyk, M. J. Med. Chem., 2012, 55, 6541-6553.
[41] Crocetti, L, Schepetkin, IA, Cilibrizzi, A, Graziano, A, Vergelli, C, Giomi, D, Khlebnikov, AI, Quinn, MT, Giovannoni, MP. J. Med. Chem., 2013, 56, 6259-6272.
[42] Lucas, SD, Gonçalves, LM, Carvalho, LAR, Correia, HF, Da Costa, EMR, Guedes, RA, Moreira, R, Guedes, RC. J. Med. Chem., 2013, 56, 9802-9806.
[43] Habash, M, Abdelazeem, A, Taha, M. Med Chem Res, 2014, 1-21.
[44] Gómez-Jeria, JS. Int. J. Quant. Chem., 1983, 23, 1969-1972.
[45] Gómez-Jeria, JS, "Modeling the Drug-Receptor Interaction in Quantum Pharmacology," in *Molecules in Physics, Chemistry, and Biology*, J. Maruani Ed., vol. 4, pp. 215-231, Springer Netherlands, 1989.
[46] Gómez-Jeria, JS, Ojeda-Vergara, M. J. Chil. Chem. Soc., 2003, 48, 119-124.
[47] Gómez-Jeria, JS, *Elements of Molecular Electronic Pharmacology (in Spanish),* Ediciones Sokar, Santiago de Chile, 2013.
[48] Gómez-Jeria, JS. Canad. Chem. Trans., 2013, 1, 25-55.
[49] Gómez-Jeria, JS, Morales-Lagos, D, "The mode of binding of phenylalkylamines to the Serotonergic Receptor," in *QSAR in design of Bioactive Drugs*, M. Kuchar Ed., pp. 145-173, Prous, J.R., Barcelona, Spain, 1984.
[50] Gómez-Jeria, JS, Morales-Lagos, D, Rodriguez-Gatica, JI, Saavedra-Aguilar, JC. Int. J. Quant. Chem., 1985, 28, 421-428.
[51] Gómez-Jeria, JS, Ojeda-Vergara, M, Donoso-Espinoza, C. Mol. Engn., 1995, 5, 391-401.
[52] Gómez-Jeria, JS, Lagos-Arancibia, L. Int. J. Quant. Chem., 1999, 71, 505-511.
[53] Gómez-Jeria, JS, Lagos-Arancibia, L, Sobarzo-Sánchez, E. Bol. Soc. Chil. Quím., 2003, 48, 61-66.
[54] Gómez-Jeria, JS, Soto-Morales, F, Larenas-Gutierrez, G. Ir. Int. J. Sci., 2003, 4, 151-164.
[55] Soto-Morales, F, Gómez-Jeria, JS. J. Chil. Chem. Soc., 2007, 52, 1214-1219.
[56] Gómez-Jeria, JS, Soto-Morales, F, Rivas, J, Sotomayor, A. J. Chil. Chem. Soc., 2008, 53, 1393-1399.
[57] Gómez-Jeria, JS. J. Chil. Chem. Soc., 2010, 55, 381-384.
[58] Bruna-Larenas, T, Gómez-Jeria, JS. Int. J. Med. Chem., 2012, 2012 Article ID 682495, 1-16.
[59] Gómez-Jeria, JS. Der Pharm. Lett., 2014, 6., 95-104.
[60] Salgado-Valdés, F, Gómez-Jeria, JS. J. Quant. Chem., 2014, 2014 Article ID 431432, 1-15.
[61] Solís-Gutiérrez, R, Gómez-Jeria, JS. Res. J. Pharmac. Biol. Chem. Sci., 2014, 5, 1401-1416.
[62] Fukui, K, Fujimoto, H, *Frontier orbitals and reaction paths: selected papers of Kenichi Fukui,* World Scientific, Singapore; River Edge, N.J., 1997.
[63] Gómez-Jeria, JS, Flores-Catalán, M. Canad. Chem. Trans., 2013, 1, 215-237.
[64] Paz de la Vega, A, Alarcón, DA, Gómez-Jeria, JS. J. Chil. Chem. Soc., 2013, 58, 1842-1851.
[65] Reyes-Díaz, I, Gómez-Jeria, JS. J. Comput. Methods Drug Des., 2013, 3, 11-21.
[66] Gómez-Jeria, JS. Int. Res. J. Pure App. Chem., 2014, 4, 270-291.
[67] Gómez-Jeria, JS. Brit. Microbiol. Res. J., 2014, 4, 968-987.
[68] Muñoz-Gacitúa, D, Gómez-Jeria, JS. J. Comput. Methods Drug Des., 2014, 4, 33-47.
[69] Muñoz-Gacitúa, D, Gómez-Jeria, JS. J. Comput. Methods Drug Des., 2014, 4, 48-63.

[70] Pino-Ramírez, DI, Gómez-Jeria, JS. Amer. Chem. Sci. J., 2014, 4, 554-575.
[71] Barahona-Urbina, C, Nuñez-Gonzalez, S, Gómez-Jeria, JS. J. Chil. Chem. Soc., 2012, 57, 1497-1503.
[72] Alarcón, DA, Gatica-Díaz, F, Gómez-Jeria, JS. J. Chil. Chem. Soc., 2013, 58, 1651-1659.
[73] Frisch, MJ, Trucks, GW, Schlegel, HB, Scuseria, GE, Robb, MA, Cheeseman, JR, Montgomery, J, J.A., Vreven, T, Kudin, KN, Burant, JC, Millam, JM, Iyengar, SS, Tomasi, J, Barone, V, Mennucci, B, Cossi, M, Scalmani, G, Rega, N. Gaussian98 Rev. A.11.3, Gaussian, Pittsburgh, PA, USA, 2002.
[74] Gómez-Jeria, JS. D-Cent-QSAR: A program to generate Local Atomic Reactivity Indices from Gaussian log files. 1.0, Santiago, Chile, 2014.
[75] Statsoft. Statistica 8.0, 2300 East 14 th St. Tulsa, OK 74104, USA, 1984-2007.
[76] Dennington, RD, Keith, TA, Millam, JM. GaussViev 5.0.8, 340 Quinnipiac St., Bldg. 40, Wallingford, CT 06492, USA, 2000-2008.
[77] Varetto, U. Molekel 5.4.0.8, Swiss National Supercomputing Centre: Lugano, Switzerland, 2008.
[78] Klopman, G. J. Am. Chem. Soc., 1968, 90, 223-234.